DOI: 10.1002/ ((please add manuscript number))
Article type: Full Paper

Title: Multiwalled Carbon Nanotubes inhibit tumor progression in a mouse model

*Lorena García-Hevia, Juan C. Villegas, Fidel Fernández, Íñigo Casafont, Jesús González, Rafael Valiente and Mónica L. Fanarraga**

Ms. Lorena García Hevia, Dr. Juan C. Villegas, Dr. Fidel Fernández, Dr. Íñigo Casafont, Dr. Jesús González, Dr. Rafael Valiente, Dr. Mónica L. Fanarraga.

Grupo de Nanomedicina-IDIVAL,
Universidad de Cantabria
Santander, 39011, Spain
E-mail: fanarrag@unican.es

Keywords: Cancer, antineoplastic agent, tubulin, anti-proliferative, biomimetic

Understanding the molecular mechanisms underlying the biosynthetic interactions between particular nanomaterials with specific cells or proteins opens new alternatives in nanomedicine and nanotoxicology. Multiwalled carbon nanotubes (MWCNTs) have long being explored as drug delivery systems and nanomedicines against cancer. There are high expectations for their use in therapy and diagnosis. These filaments can translocate inside cultured cells and intermingle with the protein nanofilaments of the cytoskeleton, interfering with the biomechanics of cell division mimicking the effect of traditional microtubule-binding anti-cancer drugs such as paclitaxel. Here we show how MWCNTs can trigger significant anti-tumoral effects *in vivo*, in solid malignant melanomas produced by allograft transplantation. Interestingly, the MWCNT anti-tumoral effects are maintained even in solid melanomas generated from paclitaxel-resistant cells. These findings provide great expectation in the development of groundbreaking adjuvant synthetic microtubule-stabilizing chemotherapies to overcome drug resistance in cancer.

1. Introduction

Carbon nanotubes (CNTs) represent a class of highly versatile materials that display very interesting mechanical, thermal, electronic and biological properties.[1] These nanomaterials have been employed, among others, as drug[2,3] or nucleic acid[4,5] delivery systems, kill cancer cells by hyperthermia,[6] or serve to detect tumors *in vivo*.[6,7] There are several studies that point at the feasibility of targeting CNTs into tumors coating these nanomaterials with different biomolecules or radicals with tropism for cancer cells such as folates, transferrin, lectin, growth factor receptors, antibodies that recognize surface tumor overexpressed proteins, etc.[6–8] CNT surface functionalization makes also possible to enhance blood circulation times, improving biodistribution and translocation into tumors.[9,10] Recently, MWCNTs have also been claimed to display intrinsic anti-proliferative,[11,12] anti-migratory[13] and cytotoxic[14–16] effects *in vitro*, resulting of the physicochemical characteristics and morphology of these nanomaterials, conferring MWCNTs remarkable biomimetic properties that prompt their association with some of the naturally-existing intracellular nanofilaments such as actin[17] or microtubules[11] that can be exploited to defeat cancer.

Microtubules are cytoskeletal polymers ubiquitous in all eukaryotic cells and key players in many cellular processes including cell division and migration. For these reasons, these protein filaments have long been considered ideal targets of many anticancer therapies including some of the most widely used drugs, such as paclitaxel (Taxol®) or the vinca alkaloids.[18] Microtubules are 25 nm diameter nanotubes, constituted of 13 tubulin protein polymers, known as protofilaments, organized in a twisted cylinder (Figure 1).[19] Interestingly, MWCNTs have been proposed as the technological counterpart of nature's microtubules for they share several aspects of their architecture and properties.[20] They both have (i) similar dimensions, (ii) a tubular morphology that ensures structural efficiency, (iii) have an analogous mechanical behaviour, and finally (iv), both structures are exceptionally resilient, *i.e.* they can be bent to a

small radius of curvature and are able to restore their original shape without damage.[21–23] However, there is a big difference between these two filaments that has chief implications in the *in vivo* system, while MWCNTs are very stable, microtubules are highly dynamic polymers that continuously undergo assembly/disassembly cycles in a process known as dynamic instability.[24] The many similarities that exist between MWCNTs and microtubules are likely to contribute to their association both, *in vitro*[25] and *in vivo*.[11] In cultured cells, tubulin and MWCNTs assemble biosynthetic microtubules that display an enhanced stability, resulting in important changes in the cell biomechanics.[11,13,26] There are many evidences in different types of cells, including cancer cells, that MWCNTs trigger several mitotic defects (aberrant spindles, chromosome mal-segregation, clastogenic effects), inhibition of cell migration, finally triggering cell death.[11,26,27] Thus *in vitro,* in cultured cells, MWCNTs mimic the effect of classic antineoplastic drugs.

Melanoma is the most aggressive type of skin cancer and although at early stages melanoma can be surgically removed, with a survival rate of 99%, metastasized melanoma is difficult to cure and has very high rates of mortality. Here we evaluate the intrinsic anti-cancer properties of MWCNTs in tumors produced by malignant melanoma allotransplantation. Among the different cancer cell models available for the study, we selected B16-F10 murine cells. These cells, as most malignant melanomas, are (i) genetically heterogeneous, (ii) highly metastatic, (iii) display an aggressive nature and (iv) are difficult to treat due to resistance.[28]

2. Results

2.1 MWCNTs translocate inside malignant melanoma cells producing cytotoxicity and interfering with cell division and spreading

To investigate the antineoplastic properties of these nanomaterials *in vivo* in melanoma cells, we first confirmed *in vitro,* in this particular cell line, MWCNT intracellular translocation.

The presence of cytoplasmic MWCNTs was investigated using transmission electron microscopy (TEM) on section of MWCNT-treated melanoma cells. As shown in Figures 2a-c MWCNTs were detectable in bundles inside the cytoplasm. Intracellular MWCNTs were further demonstrated using confocal Raman spectroscopy, focusing the laser beam within the cell cytoplasm using the Raman spectra of pristine MWCNTs and untreated cell cytoplasms as controls (Figure 2d). The typical fingerprints expected for MWCNTs were observed in the intracellular spectrum obtained from MWCNT-treated cells together with peaks that correspond to cellular proteins. Both techniques confirmed the presence of MWCNTs inside the treated cells.

Microtubule network disorganization, centrosomal disappearance, cell enlargement, nuclear heterogeneity, etc. -all indicative of the biomimetic interaction of MWCNTs with the cellular cytoskeleton as previously reported [11-13]-, were also detected in malignant melanoma treated cells (Figure 3a-c). MWCNTs also produced a patent anti-proliferative effect in these cultures resulting in statistically significantly longer cell proliferation intervals compared to untreated controls (Figures 3d, 4a), and asymmetric cell divisions or *mitotic-slippage* processes causing larger cell sizes and polyploidies (Figure 4b,Videos 1, 2). These experiments also confirmed a slower migration speed in MWCNT-treated cells (Figure 3d). In conclusion, these investigations show the susceptibility of malignant melanoma cells to the intrinsic MWCNTs antineoplastic effect *in vitro*.

2.2 Intracellular MWCNTs inhibit melanoma tumor progression *in vivo*

Many studies fail at the point of validating results *in vivo*, for solid tumors are not just disorganized masses of dividing cells that develop in different tissues. On the contrary, tumors are complex cellular structures that resemble abnormal organs, constituted of closely interrelated multiple cell types and extracellular matrix components, continuously undergoing

local tissue remodelling processes to promote malignancy compromising the host tissue.[29,30] As a tumor model, B16-F10 cells generate solid melanoma cell masses upon transplantation in the interescapular subcutaneous region of neonate mice. These tumors typically developed in 5-10 days displaying standard malignant melanoma aggressive features such as (i) a high mitotic rate, (ii) intratumoral necrotic foci, (iii) neo-vasculature development, (iv) expansive growth edges and infiltration of surrounding tissues -namely fat, muscle and peripheral nerves-, (v) and a significant inflammatory response, among others (Figure S1, Supporting Information). To investigate the effect of MWCNTs *in vivo*, we have performed two different approaches. Our first method, aiming to reduce to a maximum the natural variability and inherent noise of the *in vivo* system, consisted on a "Trojan-horse approach" where B16-F10 cells containing cytoplasmic MWCNTs were transplanted to generate solid tumors. MWCNT- cell loading was performed *in vitro*, with permissive dosages of MWCNTs (20 μg/mL) for 48 h before transplantation. These dosages and incubation times are sufficient to allow MWCNTs translocation into the cells[11,16] (Figure 1, Supplementary Figure S1), producing no detectable lethality *ex vivo* (Figure S2, Supporting Information). To ensure that control tumors developed under virtually identical conditions, littermates were simultaneously transplanted with untreated melanoma cells. The evaluation of the melanoma tumors 6 days post-transplant confirmed 60% smaller tumoral well-defined masses, displaying a solid pseudo-papillary pattern and a conspicuous acantholysis in tumors where melanoma cells had been exposed to MWCNTs (Figures 5). These results are highly indicative of the intrinsic anti-tumoral nature of MWCNTs *in vivo*.

2.3 Single intratumoral injections of MWCNTs produce significant antineoplastic effects in 96 h

There are *pros* and *cons* of the Trojan-horse approach that must be objectively taken into account. On one hand, this method circumvents the tumor targeting delivery problem, avoiding

the possible interference with the tumor microenvironment[30] while guaranteeing that most of the malignant cancer cells of the tumor mass are carriers of MWCNTs. But, on the other hand, and despite we have not observed significant cell survival differences *in vitro* at these dosages (Figure S2, Supporting Information), there is no way to guarantee that all the MWCNT-treated cells are fully viable hours after transplantation. Therefore, in order to get a picture closer to the real situation, we performed a second set of experiments consisting on a single injection of MWCNTs directly on the melanoma tumors (Figure 6). This method, although much more susceptible to biological artefacts, provides direct evidence of the intrinsic anti-tumoral effect of MWCNTs *in vivo*. For the study, we generated solid melanoma tumors that were allowed to grow for 8 days before intratumoral injection with either, serum-functionalized MWCNTs, or the MWCNT resuspension medium as a control. These intratumoral injection experiments were performed systematically in total population of more than 200 mice. The quantification and evaluation of the tumors carried out 4 days post-treatment, revealed how single intratumoral injections of 2 μg MWCNTs produced remarkable anti-tumoral effects, resulting in final tumor masses 27% smaller than those observed in untreated controls (Figures 6b-d). Examination of the tumoral tissues revealed an intense peritumoral inflammatory infiltrate, multifocal coagulation necrosis, accompanied by carbon black deposits intermingling with ghost tumoral cells displaying karyolysis i.e. the destruction of the nucleus of the cells (Figure 6e-g). In summary, the two studies using different strategies reveal that MWCNTs display intrinsic anti-tumoral effects *in vivo*, inhibiting tumor development with no aids such as accompanying drugs or interference nucleic acids. MWCNTs can significantly hinder tumor cell proliferation and spreading, preventing the growth of malignant tumor masses *in vivo*.

2.4 MWCNTs display antineoplastic effects in paclitaxel resistant melanoma cells

In the MWCNT-microtubule interaction model proposed on previous research[11,25] (Figure 1), MWCNTs intermingle with tubulin protofilaments associating along the lateral aspect of these

polymers where structural studies and theoretical calculations show that the tubulin contacts are weaker, being mostly electrostatic.[19,22] The theory underlying these results is that MWCNTs produce a scaffolding effect on microtubules that interferes with the dynamic instability that microtubules require during cell proliferation and migration.[18] Our results serve to hypothesize that this MWCNTs interaction with microtubules is likely to be compatible -and complementary- to that of traditional microtubule dynamic-interfering agents. These drugs, namely taxanes (paclitaxel, docetaxel and cabazitaxel), promote microtubule stabilization inhibiting the disassembly of the tubulin polymer, binding to a lateral region localized in the polymerized β-tubulin molecule.[31] In malignant cancer cells, this small structural interaction pocket is subject of different mutations and post-translational changes that result in resistance to chemotherapy.[32] To validate our MWCNT-microtubule interaction model, we complemented these results testing the MWCNT anti-tumoral effect on paclitaxel-resistant tumors. For the study, we treated cultures of melanoma cells with 40 μM paclitaxel, killing most cells in the culture (Figure 7a, Supplementary Figure S3). Approximately 4 weeks after the original treatment, the few surviving cell colonies were isolated and amplified *in vitro* (Figure 7b). These resistant cells were finally transplanted to generate solid tumors following the above protocol. As hypothesized, paclitaxel-resistant melanoma tumors were also 45% smaller after one single injection treatment with 2 μg of MWCNTs (Figure 7c). These results suggest a significant adjuvant effect of MWCNTs on paclitaxel-resistant tumors.

3. Conclusion

Here we demonstrate how MWCNTs have intrinsic antineoplastic properties, triggering anti-proliferative and cytotoxic effects in highly aggressive recurrent and heterogeneous neoplasias such as malignant melanomas very difficult to treat with conventional chemotherapies such as paclitaxel.[28] These results serve to conjecture that MWCNTs can represent a new ground-breaking type of synthetic microtubule-stabilizing agents that could be used as adjuvant or

neoadjuvant treatments to enhance the effect of the traditional tubulin binding chemotherapies, preventing drug resistance in cancer cells. In addition, MWCNTs might also have a "spin-off effect" eliminating the tumoral stromal cells that sustain cancer cell growth, invasion and metastasis, displaying additional attractive therapeutic advantages, since destroying the supporting cells in the tumor is likely to reduce the risk of resistance and recurrence.[30] Our data pioneer radically new strategies in the design of synthetic microtubule-stabilizing agents for cancer treatment.

4. Experimental Section

MWCNTs characterization, functionalization and dispersion: MWCNTs were synthesized following the catalytic CVD method as previously described.[33] The characterization of the *as-produced* MWCNTs can be found in Figure S4 (Supporting Information) and can be complemented with previous reports.[11] The unpolarized Raman spectra were taken at room temperature with a Horiba T64000 triple spectrometer in the backscattering geometry, using the 514 nm line of a Coherent Innova Spectrum 70C Ar^+–Kr^+ laser and a nitrogen cooled CCD (Jobin-Yvon Symphony) coupled to a confocal microscope for detection. The laser beam was focused down to 1 μm spot with a 100x objective and kept the power on the sample below 2 mW to avoid laser-heating effects on the probed material and the concomitant softening of the observed Raman peaks. MWCNTs produce a characteristic Raman spectrum distinguishable from the SWCNT spectrum. The radial breathing modes (RBM), a Raman feature associated to the inner diameter, are not common and can only sometimes be observed when a good resonance condition is established. The RBM signal from large diameter tubes is usually too weak to be observable and the ensemble average of inner tube diameter broadens the signal. The intracellular Raman spectra were obtained in fixed cells focusing the laser beam in a cytoplasmic Z position at 1-5 μm from the cell basement. The as-produced MWCNTs were resuspended in standard tissue culture medium containing serum

after repeated cycles of vortex mixing followed by mild sonication. The MWCNT concentration was quantified by optical absorption at 550 nm. A 0.2 mg/mL MWCNTs stock solution was prepared to be diluted in standard culture medium to the indicated final working solution.

Cell culture: B16-F10 murine malignant melanoma cells (ATCC® CRL-6475™) were cultured in Iscove´s Dulbecco's Modified Medium 10% serum containing antibiotics. These cells, as most malignant melanomas, are genetically heterogeneous, highly metastatic, display an aggressive nature and are difficult to treat due to resistance.[34] Paclitaxel-resistant melanoma cell colonies were observed 4 weeks after a 4-day paclitaxel cytotoxic treatment. These paclitaxel-resistant cell colonies were amplified *in vitro* to generate paclitaxel-resistant cultures that were used for allotransplantation.

Solid melanoma tumor growth studies: All animal experimentation procedures were performed humanely, according to EU legislation following the principle of the "Three Rs", to Replace, Reduce and Refine the use of animals. Tumorigenesis was induced by subcutaneous transplantation of a total of 2×10^5 B16-F10 melanoma cells in 10 µL of IMDM 10% serum. The under-developed immune system in neonate mice,[35] together with the growth factor and hormonal conditions in their tissues ensure a perfect environment to support solid pigmented tumors, which are developed in 5-10 days. In all the experimental approaches, littermates were injected in parallel to controls. This allowed to observe each litter as a single experiment by itself. In the Trojan horse approach, cells were incubated during 48 h with 20 µg/mL of MWCNTs added to the tissue culture medium. Cell viability and cell cycle analysis were validated for each transplant using the trypan blue exclusion assay. Tumors were allowed to grow for 6 days before analysis. For the intratumoral injection approach, solid melanomas were allowed to grow for 9 days before injection directly in the tumor masses of 2 µg of MWCNTs resuspended in a volume of 10 µL of culture medium. Control littermates bearing identical tumors were injected with the resuspension medium. Three days post injection tumors were analyzed. In both experimental approaches, tumor masses were carefully dissected, weighed,

fixed and dehydrated for paraffin sectioning, hematoxylin-eosin staining, and further analysis. Histological analysis was carried out in 4% formalin fixed tissues, buffered and dehydrated for paraffin sectioning and further hematoxylin-eosin staining for analysis. Carbon aggregates shown in Figure 6g were revealed in paraffin tissue sections treated with hydrogen peroxide to remove melanin.

Statistical Analysis: A *t*-test statistical analysis was carried out to evaluate the significance of results. The confidence level and total number of events included in the study are indicated for each statistical analysis. Quantitative results are expressed as mean values with their corresponding standard deviation error bars.

Flow Cytometry: It was used to perform quantitative and qualitative analysis of the total DNA content per cell, in approximately 10.000 cells per condition. This allows the simultaneous determination of the percentages of cells at each stage of the cell cycle, and the percentage of apoptotic cells. Flow cytometry was performed on a suspension of fixed cells stained with Hoechst dyes (Bisbenzimide) using a Becton Dickinson FACS CantoII equipment. Data were analyzed using the FACS Diva software (Becton Dickinson, NJ, USA).

Time-lapse video microscopy, Immunostaining and Confocal Microscopy Imaging: Time-lapse films were performed during 12 h in a Nikon Eclipse Ti-live-cell station. Movies (supplementary video#1, #2, #3) were obtained at 15 min/frame using a 10x Nikon N.A. 0.45. Quantification analysis was performed with the NIS-Elements software. Immunostaining was performed in cells were fixed in 4% paraformaldehyde as described elsewhere.[11] The anti-α-tubulin (B512) (Sigma-Aldrich) was combined with a secondary goat anti-mouse IgG antibody conjugated with Alexa Fluor 488 (Molecular Probes, Invitrogen). Actin was stained with phalloidin-tetramethylrhodamine B isothiocyanate (Sigma-Aldrich) and DNA (nucleus and chromosomes) with Hoechst dye (Sigma-Aldrich). Confocal microscopy images were obtained with a Nikon A1R confocal microscope. All confocal cell images are pseudo-colored.

Supporting Information

Supporting Information is available from the Wiley Online Library or from the author.

Acknowledgements
We thank Dr. E. Flahaut for providing the MWCNTs. We are grateful to the Nikon A1R Laser Microscopy Unit of the IDIVAL Institute for the electron microscopy and confocal/time-lapse microscopy, and to M. Aramburu and J. Díaz-Gómez for their help. This work has been supported by the Spanish MINECO and European Union FEDER under Projects ref. PI13/01074 (AES 2013) and MAT2012-38664-C02-01. We especially thank the Fundación Eugenio Rodríguez Pascual (ref "Ayudas de investigación" 2014).

References

[1] M. F. L. De Volder, S. H. Tawfick, R. H. Baughman, a J. Hart, *Science* **2013**, *339*, 535.

[2] M. Adeli, R. Soleyman, Z. Beiranvand, F. Madani, *Chem. Soc. Rev.* **2013**, *42*, 5231.

[3] M. Das, S. R. Datir, R. P. Singh, S. Jain, *Mol. Pharm.* **2013**, *10*, 2543.

[4] R. Krajcik, A. Jung, A. Hirsch, W. Neuhuber, O. Zolk, *Biochem. Biophys. Res. Commun.* **2008**, *369*, 595.

[5] S. Foillard, G. Zuber, E. Doris, *Nanoscale* **2011**, *3*, 1461.

[6] K. Kostarelos, A. Bianco, M. Prato, *Nat. Nanotechnol.* **2009**, *4*, 627.

[7] J. J. Mulvey, C. H. Villa, M. R. McDevitt, F. E. Escorcia, E. Casey, D. a Scheinberg, *Nat. Nanotechnol.* **2013**, *8*, 763.

[8] A. A. Bhirde, V. Patel, J. Gavard, G. Zhang, A. A. Sousa, A. Masedunskas, R. D. Leapman, R. Weigert, J. S. Gutkind, J. F. Rusling, *ACS Nano* **2009**, *3*, 307.

[9] H. Ali-Boucetta, K. Kostarelos, *Adv. Drug Deliv. Rev.* **2013**, *65*, 2111.

[10] B. R. Smith, E. E. B. Ghosn, H. Rallapalli, J. a Prescher, T. Larson, L. a Herzenberg, S. S. Gambhir, *Nat. Nanotechnol.* **2014**, *9*, 481.

[11] L. Rodriguez-Fernandez, R. Valiente, J. Gonzalez, J. C. Villegas, M. L. Fanarraga, *ACS Nano* **2012**, *6*, 6614.

[12] L. M. Sargent, a. F. Hubbs, S. H. Young, M. L. Kashon, C. Z. Dinu, J. L. Salisbury, S. a. Benkovic, D. T. Lowry, a. R. Murray, E. R. Kisin, K. J. Siegrist, L. Battelli, J. Mastovich, J. L. Sturgeon, K. L. Bunker, a. a. Shvedova, S. H. Reynolds, *Mutat. Res. - Genet. Toxicol. Environ. Mutagen.* **2012**, *745*, 28.

[13] L. Garcia-Hevia, R. Valiente, J. L. Fernandez-Luna, E. Flahaut, L. Rodriguez-Fernandez, J. C. Villegas, J. Gonzalez, M. L. Fanarraga, *Adv. Healthc. Mater.* **2015,** *4,* 1640.

[14] Y.-Y. Guo, J. Zhang, Y.-F. Zheng, J. Yang, X.-Q. Zhu, *Mutat. Res.* **2011**, *721*, 184.

[15] L. Ju, G. Zhang, X. Zhang, Z. Jia, X. Gao, Y. Jiang, C. Yan, P. J. Duerksen-Hughes, F. F. Chen, H. Li, X. Zhu, J. Yang, *PLoS One* **2014**, *9*.

[16] L. García-Hevia, R. Valiente, J. González, H. Terán, J. L. Fernández-Luna, J. C. Villegas, M. L. Fanarraga, *Curr. Pharm. Des.* **2015**, *21*, 1920.

[17] B. N. Snyder-Talkington, D. Schwegler-Berry, V. Castranova, Y. Qian, N. L. Guo, *Part. Fibre Toxicol.* **2013**, *10*, 35.

[18] M. A. Jordan, L. Wilson, *Curr. Opin. Cell Biol.* **1998**, *10*, 123.

[19] E. Nogales, M. Whittaker, R. A. Milligan, K. H. Downing, *Cell* **1999**, *96*, 79.

[20] F. Pampaloni, E. L. Florin, *Trends Biotechnol.* **2008**, *26*, 302.

[21] P. Williams, S. J. Papadakis, M. Patel, M. R. Falvo, S. Washburn, R. Superfine, *Phys. Rev. Lett.* **2002**, *89*, 255502.

[22] V. VanBuren, D. J. Odde, L. Cassimeris, *Proc. Natl. Acad. Sci. U. S. A.* **2002**, *99*, 6035.

[23] P. J. de Pablo, I. A. T. Schaap, F. C. MacKintosh, C. F. Schmidt, *Phys. Rev. Lett.* **2003**, *91*, 098101.

[24] T. Mitchison, M. Kirschner, *Nature 312*, 237.

[25] C. Z. Dinu, S. S. Bale, G. Zhu, J. S. Dordick, *Small* **2009**, *5*, 310.

[26] K. J. Siegrist, S. H. Reynolds, M. L. Kashon, D. T. Lowry, C. Dong, A. F. Hubbs, S.-H. Young, J. L. Salisbury, D. W. Porter, S. A. Benkovic, M. McCawley, M. J. Keane, J. T. Mastovich, K. L. Bunker, L. G. Cena, M. C. Sparrow, J. L. Sturgeon, C. Z. Dinu, L. M. Sargent, *Part. Fibre Toxicol.* **2014**, *11*, 6.

[27] L. Gonzalez, I. Decordier, M. Kirsch-Volders, *Biochem. Soc. Trans.* **2010**, *38*, 1691.

[28] P. Hersey, X. D. Zhang, *Nat. Rev. Cancer* **2001**, *1*, 142.

[29] M. Egeblad, E. S. Nakasone, Z. Werb, Tumors as organs: Complex tissues that interface with the entire organism. *Dev. Cell* **2010**, *18*, 884–901.

[30] D. Quail, J. Joyce, *Nat. Med.* **2013**, *19*, 1423.

[31] C. Alberti, *Eur. Rev. Med. Pharmacol. Sci. 13*, 13.

[32] G. Orr, P. Verdier-Pinard, H. McDaid, S. B. Horwitz, *Oncogene* **2003**, *22*, 7280.

[33] E. Flahaut, C. Laurent, A. Peigney, *Carbon N. Y.* **2005**, *43*, 375.

[34] G. Poste, J. Doll, I. R. Hart, I. J. Fidler, *Cancer Res.* **1980**, *40*, 1636.

[35] K. S. Landreth, *Hum. Exp. Toxicol. 21*, 493.

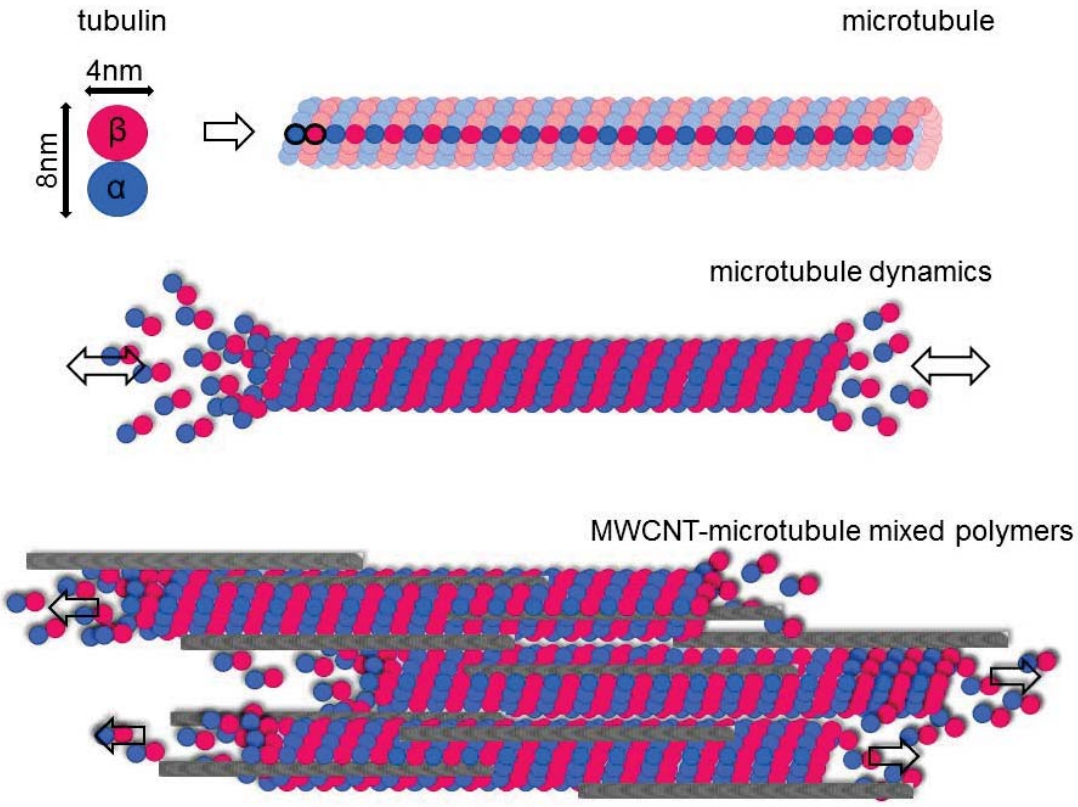

Figure 1. Microtubule-MWCNT interaction model. Microtubules are tubular polymers assembled of 13 protofilaments constituted of αβ-tubulin subunits aligned in a head-to-tail fashion. Microtubules display a high dynamicity both *in vitro* and *in vivo*. Microtubule depolymerization results of structural conformational changes in the αβ-tubulin molecule that destabilize the polymer. Intracellular MWCNTs associate with microtubules, stabilizing the tubulin polymers, interfering with the cell cytoskeleton function. This model is based on previous research.[11,25]

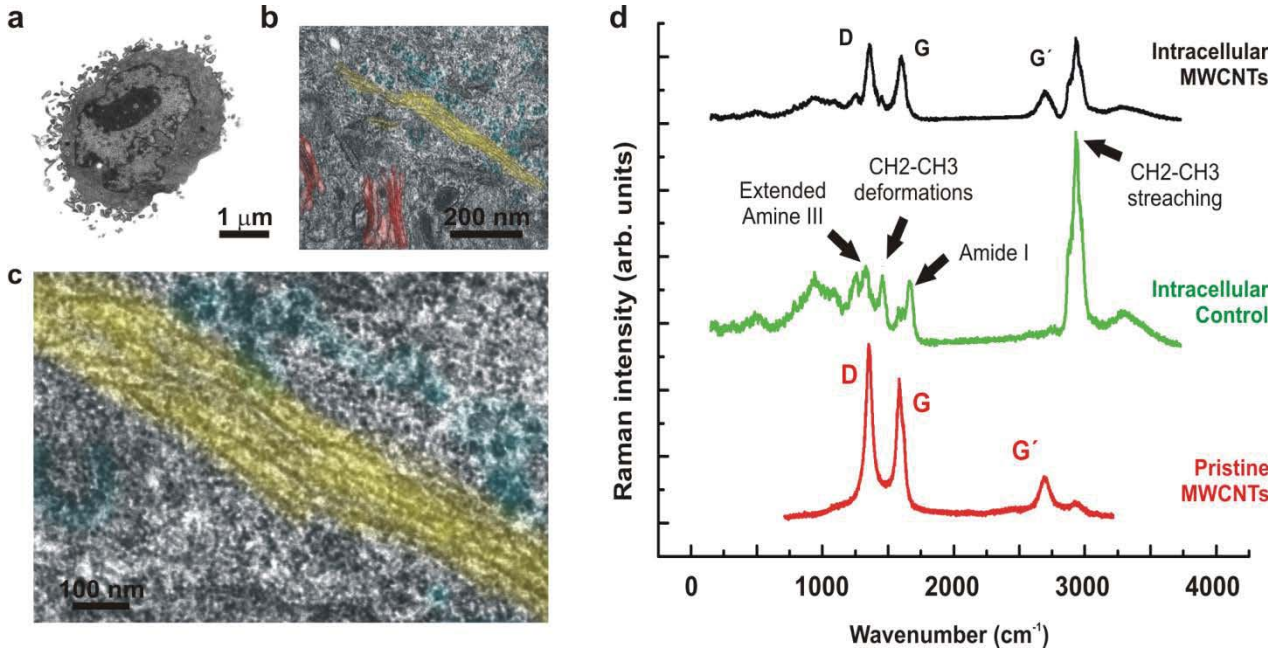

Figure 2. MWCNTs translocate inside malignant melanoma cells. a) Electron microscopy image of a cytoplasmic section of a B16-F12 melanoma cell treated *in vitro* with MWCNTs. b) High magnification image of the cytoplasm of the cell displaying MWCNTs (pseudo-colored in yellow). The Golgi membrane stacks and the ribosome-rich regions are pseudo-colored in red and blue respectively. c) Intracellular bundles of MWCNTs filaments measuring an average of 6 nm diameter. d) Raman scattering experiments performed on pristine MWCNTs (red), untreated cell cytoplasms as a control (green), and the cytoplasm of a 48 h MWCNT-treated melanoma cell (black). The spectra of pristine MWCNTs display the typical fingerprints expected for MWCNTs -indicated as D, G and G'-. These peaks specific of MWCNTs that are also observed in the intracellular spectrum obtained from MWCNT-treated cells (black) together with characteristic peaks that correspond to cellular proteins, confirm the presence of cytoplasmic MWCNTs.

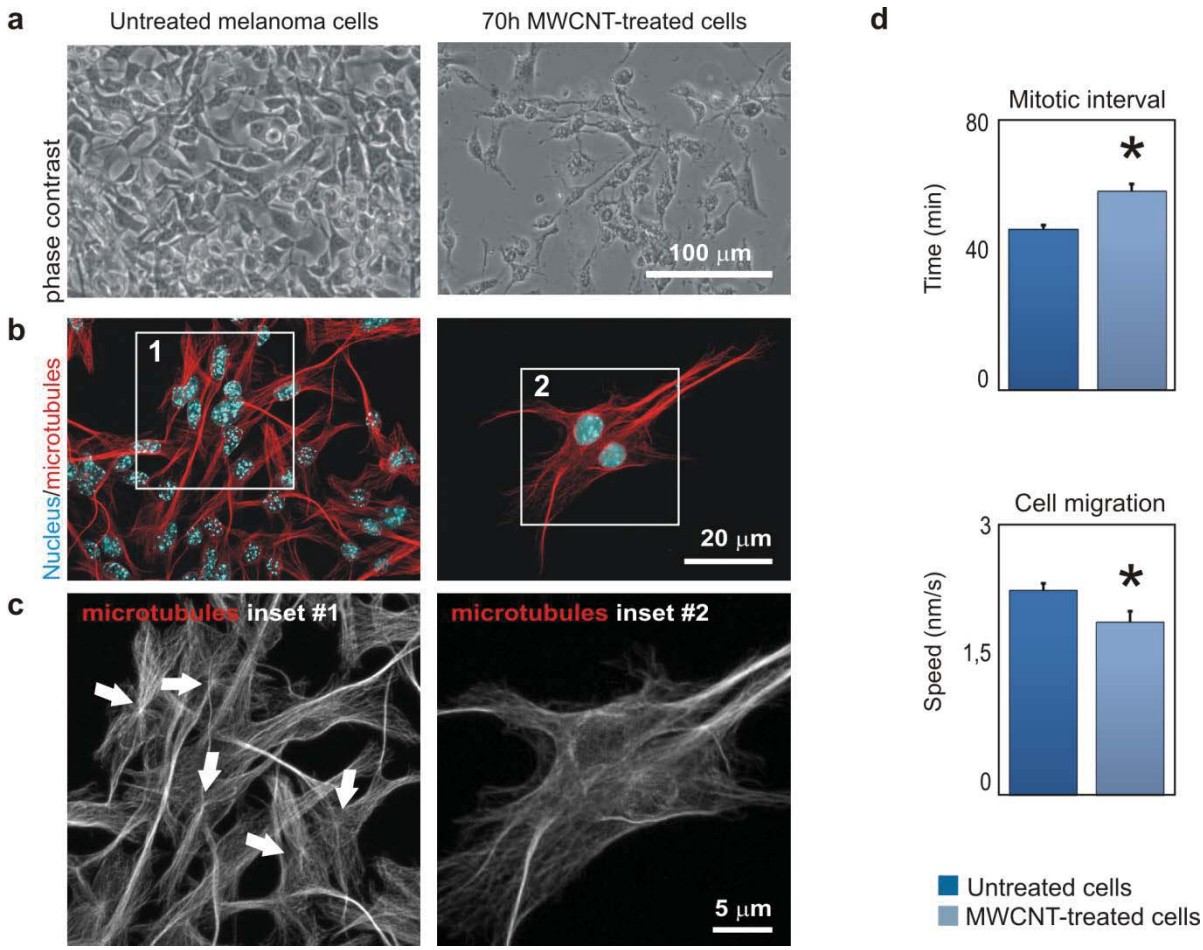

Figure 3 . MWCNTs display antineoplastic effects *in vitro*. a) Phase contrast image of control melanoma cells and MWCNT-treated cultures exposed to 100 μg/mL MWCNT for 70 h. A significantly decreased cell population together with characteristic cytotoxic features are evident in MWCNT-treated cells. b) Confocal microscopy projection images of melanoma cells displaying labelled nuclei (blue channel) and microtubules (red channel). MWCNT-treated cells (right) are larger in size, and display a poorly organized microtubule network. c) High magnification of the microtubule cytoskeleton networks shown in Figure 1b. Untreated melanoma cells (inset #1) display an evident microtubule radial organization with visible centrosomes in most cells (arrows). MWCNT-treated cells (inset #2) display a disorganized microtubule network with no observable centrosomes. d) MWCNT-treated cells have statistically longer proliferation cycles (metaphase to telophase) (t = 4.088; n= 270; *confidence level* 99.9%) and slower migration speeds (t = 2.4; n= 176; *confidence level* 98%).

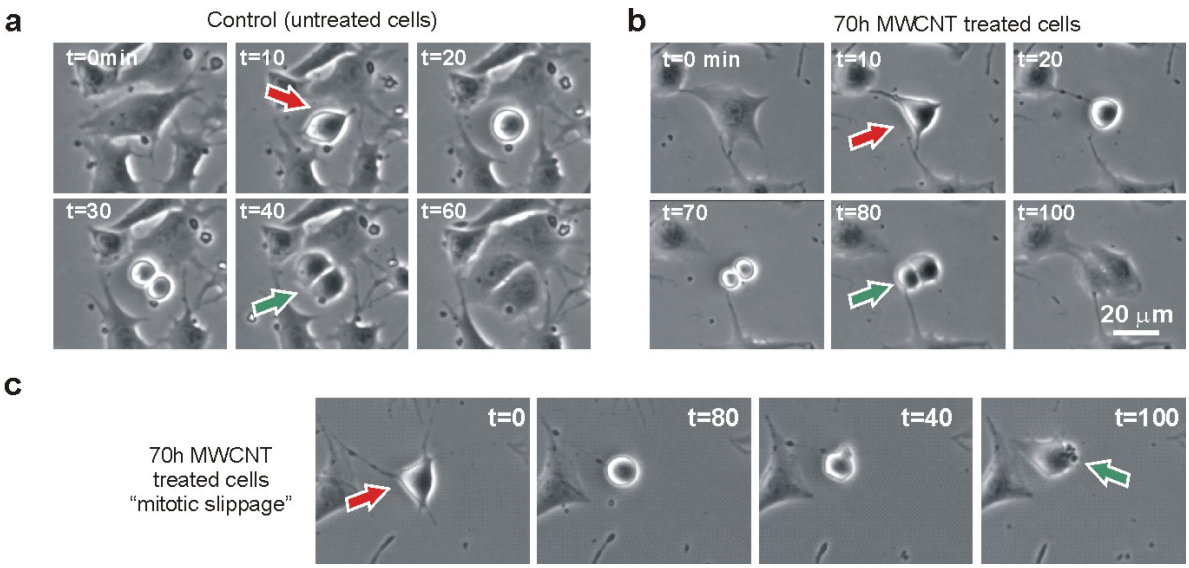

Figure 4. MWCNTs interfere with malignant melanoma cell proliferation in vitro. a) Time-lapse photograms of a representative melanoma cell mitotic cycle, from metaphase (red arrow) to telophase (green arrow). Time point intervals are shown on the top of each image. b) Photograms of a representative MWCNT-treated cell mitotic cycle. Melanoma cells exposed to MWCNTs undergo significant delays in the cell division process often resolving in asymmetric cell divisions. These images correspond to video S1 (Supporting information). c) MWCNT-treated cell mitotic cycle photograms. This cell division exit bypasses the G2 mitotic arrest by a mechanism known as "mitotic slippage". This abnormal mitotic exit leads to larger cell sizes and polyploidies as observed in MWCNT-treated cultures. This drug resistance mechanism resulting in polyploidy is frequently employed by malignant cancer cells exposed to microtubule stabilizing drugs such as paclitaxel. These images correspond to video S2 (Supporting information).

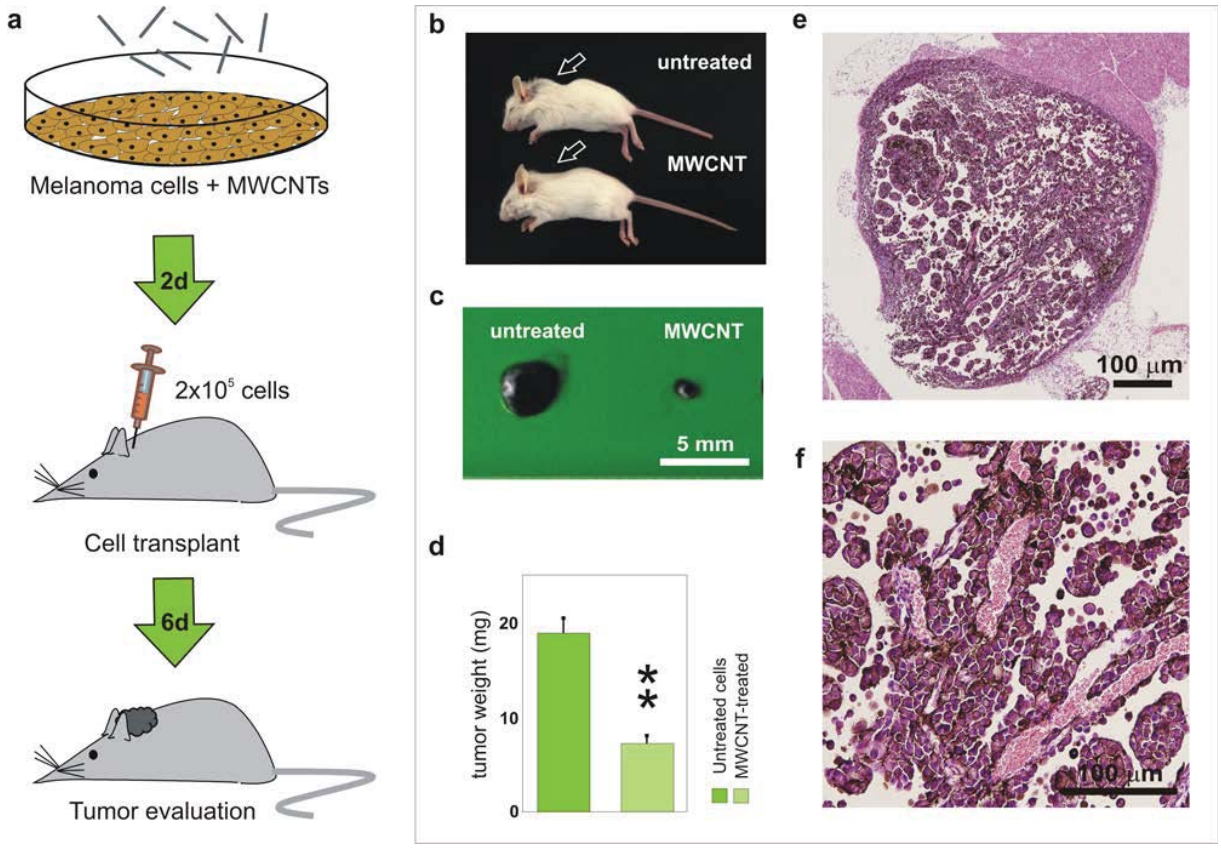

Figure 5. Antineoplastic effect of MWCNTs in solid tumors using the "Trojan Horse" approach. a) Diagram of the "Trojan-horse" approach". A total of 2×10^5 malignant melanoma cells pre-incubated with 20 μg/mL of MWCNTs or untreated controls were transplanted into host mice. Tumors were allowed to grow for 6 days before evaluation. b) Representative mouse littermates used for the experiment, MWCNT-treated melanoma cells produce smaller tumors (arrows) than control untreated cells. c) Representative solid melanoma tumoral masses. d) Statistical analysis of the antineoplastic effect of intracellular MWCNTs. The average tumoral mass weight was significantly smaller when melanoma cells were pre-treated with MWCNTs (t = 5.38; n = 77; *confidence level* >99.9%). e) Hematoxylin-eosin section of tumor displaying a non-infiltrating tumoral cell mass of pigmented epithelial melanoma cells typically packed into small well-defined masses, presenting a solid pseudo-papillary pattern and acantholysis (loss of intercellular connections) around blood vessels. f) Detail of the acantholysis surrounding small blood vessels loaded with visible erythrocytes.

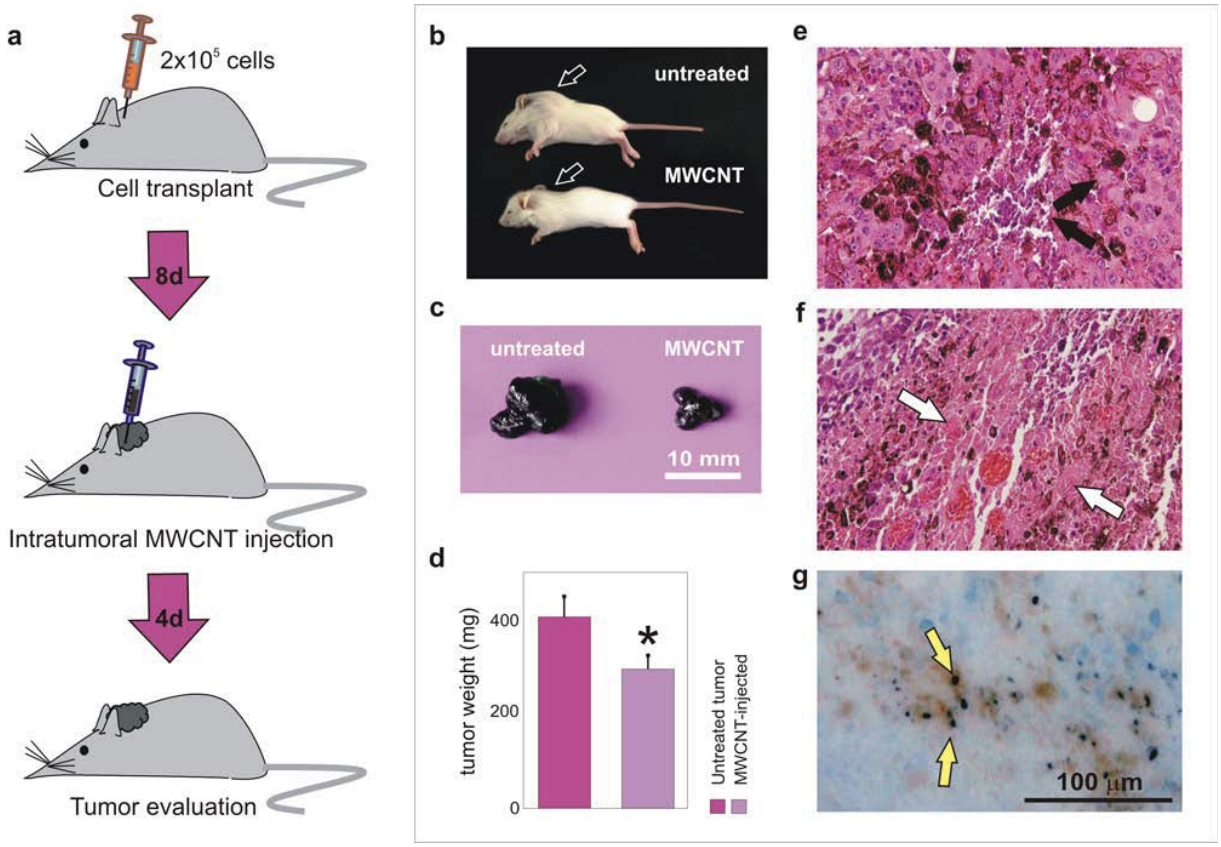

Figure 6. Antineoplastic effect of MWCNTs in solid tumors. a) Diagram of the intratumoral MWCNTs injection approach. A total of 2×10^5 melanoma cells were transplanted per mouse as described. Allotransplants were allowed to grow for 8 days before intratumoral MWCNTs injection. Solid melanomas were evaluated 4 days post-MWCNTs treatment. b) Representative mouse littermates used for the experiment. MWCNT-injected mice display smaller tumors than controls (arrows). c) Representative solid melanoma tumoral masses. d) Statistical analysis of the effect of single MWCNTs intratumoral injections. The average tumoral size was significantly smaller in MWCNTs treated tumors (t= 1.85; n= 161; *confidence level*= 95%). e) Hematoxylin-eosin section of MWCNT-injected melanoma tumors. Circumscribed tumoral masses displayed an intense peritumoral inflammatory infiltrate, multifocal necrosis that displayed dystrophic calcification and carbon black deposits that were often intermingling with melanin in pigmented cells. f) Detail of Fig 3e. Brown pigmented epithelial cells intermingle with areas of coagulation necrosis (black arrow) and ghost cells displaying karyolysis (white arrows) in the tumor. g) Intratumoral MWCNTs black-carbon deposits (yellow arrows).

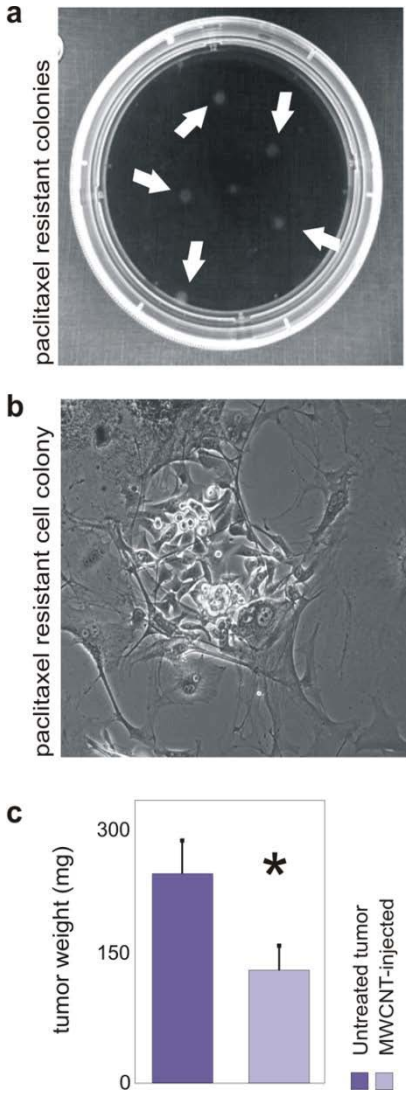

Figure 7. MWCNT adjuvant effect on paclitaxel resistant cells *in vivo*. a) Surviving paclitaxel-resistant melanoma cell colonies 4 weeks after a 4-day paclitaxel cytotoxic treatment. b) Phase contrast image of a single paclitaxel-resistant cell colony before cellular amplification. c) Statistical analysis of the effect of MWCNTs single injections in tumors generated with paclitaxel-resistant melanoma cells. The average final tumoral size was significantly smaller in tumors treated with MWCNTs ($t = 1.81$; $n = 74$ *confidence level* = 95%).

TOC

Overcoming resistance to chemotherapy requires radically new alternatives to traditional drugs. MWCNTs and microtubules share many properties that prompt their intracellular association producing antineoplastic effects in cultured cancer cells. Here it is shown how single intratumoral doses of serum-functionalized MWCNTs produce significant anti-tumoral effects even in paclitaxel-resistant tumors. Thus MWCNTs represent a possible solution for new generation microtubule-binding anti-cancer agents.

Keyword: Cancer, antineoplastic agent, tubulin, anti-proliferative, biomimetic

Lorena García Hevia, Juan C. Villegas, Fidel Fernández, Íñigo Casafont, Jesús González, Rafael Valiente and Mónica L. Fanarraga*.

Title: Multiwalled Carbon Nanotubes inhibit tumor progression in a mouse model

ToC figure